

THE DETECTIVE QUANTUM EFFICIENCY OF COMPUTED TOMOGRAPHIC (CT) RECONSTRUCTION: THE DETECTION OF SMALL OBJECTS*

K. M. Hanson

University of California, Los Alamos Scientific Laboratory
Los Alamos, NM 87545

Abstract

The loss of detection sensitivity incurred by any stage of image processing may normally be characterized by the frequency dependence of the detective quantum efficiency (DQE) of that stage of processing, provided the image is represented in continuous coordinates. However, limitations to the DQE concept arise when discretely sampled projection data are used to obtain discretely sampled computed tomographic (CT) reconstructions. The source of these limitations is the aliasing produced by the discrete sampling which mixes contributions from various frequencies. An associated problem is that the SNR for the detection of an object can depend upon the position of the object relative to the discrete reconstruction pixels. The effective SNR for discrete images must take into account this variation. While there may be no loss in the detection SNR for reconstructions in continuous coordinates (DQE = 100%!), a reduction in the SNR will result from aliasing for discrete reconstructions. A simple one-dimensional model elucidates the characteristics of discrete CT reconstruction.

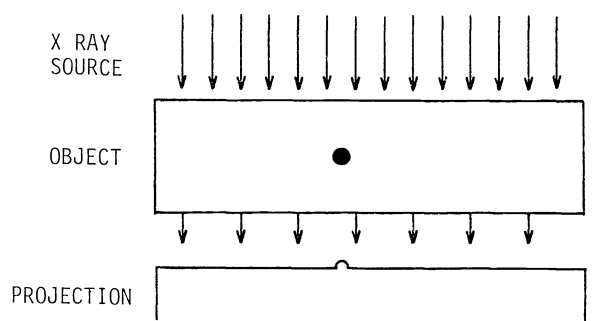
Introduction

The problem of the detection of objects in statistically limited computed tomographic (CT) reconstructions has been approached by several authors.¹⁻⁴ These authors have mainly dealt with effect of the unusual correlations in CT noise⁵⁻⁷ on the detection of reconstructed objects. Their derivations, based on continuous coordinates, have thus far avoided the question of the effect of discrete reconstructions on detection. This paper will concentrate on these effects which will become especially important for the detection of small objects (i.e., smaller than a few pixels width). A one-dimensional model of the CT reconstruction process will be used to demonstrate the types of effects that can be expected to occur in the standard 2-D (or 3-D) CT reconstruction. The results for the 1-D model are directly applicable to situations in which discrete 1-D signals are combined to improve the signal-to-noise ratio.

One-Dimensional Case

1-D Model

A one-dimensional model will be used to illustrate the effects of discrete sampling. Figure 1 presents the hypothetical x-ray radiographical situation. A source of x rays illuminates a section of uniform background material in which is embedded the object to be detected. The integral of the combined attenuation coefficient through the material, called the projection, is



$$p(x) + p_0 = \ln \frac{N_0(x)}{N(x)} \quad (1)$$

where $N_0(x)$ is the initial x-ray density and $N(x)$ is the unscattered x-ray density. $p(x)$ is the contribution from the object and p_0 is the constant contribution from the background material. The noise power spectrum of the measured projections arising from the statistical fluctuations in the number of detected x rays is

$$S_p(f) = \frac{1}{N} \quad (2)$$

Fig. 1 One-dimensional model for the detection of an object.

where N is the average density of unscattered

* Work supported by the U. S. Department of Energy

x rays assuming $N_o \gg N$ and 100% detection efficiency. From signal detection theory we know that the optimum signal-to-noise ratio for the detection of the object is⁹

$$\text{SNR}^2 = \int df \frac{|P(f)|^2}{S_p(f)} = \int df \text{PSNR}(f) \quad (3)$$

$$= N \int df |P(f)|^2 \quad (4)$$

where $P(f)$ is the Fourier transform of the projection of the object. PSNR stands for the power signal-to-noise ratio. It is well to point out that this SNR applies to the binary decision case in which the decision to be made is whether or not a specific signal is present at a specific location. In this situation the SNR is the same as the detection sensitivity index d' used to describe the resulting receiver operated characteristic (ROC) curves.⁹ The optimum SNR is that achieved by the optimum receiver (or decision criterion), in which the characteristics of the noise as represented by S_p are taken into account. The optimum receiver is equivalent to the well-known matched filter¹⁰ method. Equations 3 and 4 assume that there is no degradation of the projection signal in the imaging process (MTF = 1).

Discrete Projections

We now augment the 1-D model by supposing that the projections are sampled discretely instead of continuously. Thus, the measurements consist of a sequence of values each of which correspond to the number of x rays accumulated within an integrating aperture centered on a given position. It is assumed that the positions of these measurements are evenly distributed along the x-axis with spacing a . The effect of the aperture may be considered equivalent to a convolution of the original projection $p(x)$ with the aperture function $g(x)$. The Fourier transform of the discretely sampled projections is

$$P_{y_o}^D(f) = G(f) P(f) e^{i2\pi f(\Delta - y_o)} * \sum_{k=-\infty}^{\infty} \delta(f - 2kf_a) \quad (5)$$

The exponential phase factor results from the offset of the sampling grid relative to $x = 0$ by a distance y_o . Also, Δ is the position of the object relative to $x = 0$, and $P(f)$ is the Fourier transform of the object centered at the origin. The convolution (*) with the sequence of δ -functions represents the well-known aliasing effect¹¹ which is produced by discrete sampling. The discrete sampling at a spacing a can only represent frequencies up to the Nyquist frequency $f_a = (2a)^{-1}$. Thus, contributions present in the distribution being sampled which occur at frequencies above f_a must reappear below f_a . A convenient notation for this aliasing convolution operation is^a

$$A_{f_a}\{q(f)\} = \sum_{k=-\infty}^{\infty} \delta(f - 2kf_a) * q(f) = \sum_{k=-\infty}^{\infty} q(f - 2kf_a) \quad (6)$$

Then Eq. 5 may be written as

$$P_{y_o}^D(f) = A_{f_a}\{G(f) P(f) e^{i2\pi f(\Delta - y_o)}\}, |f| \leq f_a \quad (7)$$

The noise power spectrum of the discretely sampled projections is unaffected by the sampling aperture since the x rays detected in each measurement are independent of those detected in other measurements. Thus, the noise fluctuations are uncorrelated leading to a flat noise spectrum (white noise)

$$S_p^D(f) = \frac{1}{N}, \quad |f| \leq f_a \quad (8)$$

where N' is the number of x rays detected per unit distance in each projection. Note that N' need not be equal to N since the detection efficiency may not be 100%. Also, it should be realized that this spectrum is only defined for $|f| \leq f_a$, as in Eq. 7, not over the whole frequency range as in Eq. 2.

In order to extend this model to simulate the normal 2-D CT case we will assume that many projection measurements are made, each with a different position of the sampling grid y_o . For example, Fig. 2 illustrates four projections taken of a point object with a rectangular aperture function of width a . If the set of m projections taken at various values of y_o are used to detect the presence of the object, the optimum SNR is simply:

$$\begin{aligned} \text{SNR}_p^2 &= \sum \text{SNR}_p^2(y_o) \\ &= \sum \int_{-f_a}^{f_a} df \frac{|P_{y_o}(f)|^2}{S_p^D(f)} \\ &= \int_{-f_a}^{f_a} df \frac{\sum |P_{y_o}(f)|^2}{S_p^D(f)} \end{aligned} \quad (9)$$

It is found that in the limit as m goes to infinity, the integral of Eq. 9 may be written as:

$$\text{PSNR}_p^D(f) = mN' A_{f_a} \{|G(f)|^2 |P(f)|^2\} = \text{NEQ} A_{f_a} \{|G|^2 |P|^2\} \quad , |f| \leq f_a \quad (10)$$

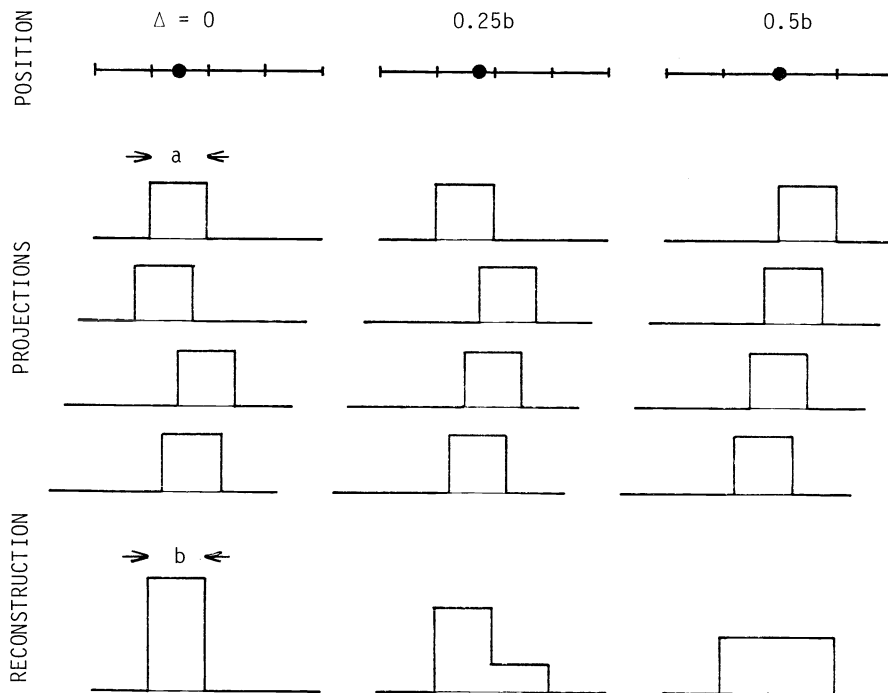


Fig. 2 Example of discrete projections obtained in the 1-D model for three different positions (Δ) of a point object. A rectangular aperture function is assumed. The reconstruction is produced by backprojection using nearest-neighbor interpolation with the same sample spacing as the projections.

The interesting aspect of this equation is that when the signal power is averaged over all y_0 the offset phase factor in Eq. 7 eliminates those amplitude products which occur at different aliased frequencies. Thus, the PSNR for the discretely sampled projections is just the aliased product of object and aperture power spectra divided by the noise power spectrum. The product mN' has been replaced by NEQ , the total number of noise equivalent quanta detected per unit distance for all of the projections. We see that NEQ plays a central role in the detection capabilities inherent in the projection data.

It is interesting to analyze the projections depicted in Fig. 2 in terms of the foregoing. Since the object is assumed to be a δ -function, $P(f) = P_0 = \text{constant}$. Also, the Fourier transform of the rectangular aperture function is $G(f) = \text{sinc} \frac{\pi f}{2f_a}$ where $\text{sinc } z = z^{-1} \sin z$. Then,

$$\begin{aligned} \text{PSNR}_p^D(f) &= NEQ \cdot P_0^2 A_{f_a} \left\{ \text{sinc}^2 \frac{\pi f}{2f_a} \right\} \\ &= NEQ P_0^2 \end{aligned} \quad (11)$$

since when the sinc^2 function is aliased, the result is unity. Equation 11 indicates that PSNR is independent of frequency. But this is what is expected since the projections are δ -functions in their discrete representation leading to a constant signal power in frequency space.

Discrete Reconstruction

To mimic 2-D CT reconstruction one step further, let us suppose that we wish to combine all of the projection measurements into a single 1-D distribution which we will call a "reconstruction." It is desirable to maintain the SNR for the detection of the object as much as possible. However, we will suppose that we are constrained to a discrete representation for the reconstruction. An appropriate algorithm for the reconstruction process is that of backprojection. In backprojection, the contribution at a specific point in the reconstruction is proportional to the sum of the values of the projections at that same position. Since the projection measurements are only known at discrete positions, some method of interpolation between these positions is required. If nearest-neighbor interpolation is employed, the interpolation function $h(x)$ is merely a rectangular function of width a . The Fourier transform of the interpolated projection is

$$P_{y_0}^I(f) = H(f) P_{y_0}^D(f) \quad (12)$$

where $H(f)$ is the Fourier transform of the interpolation function $h(x)$. If the projections are to be filtered before backprojection, the effect of the filter may be readily incorporated in $H(f)$. For the 1-D model at hand, filtering is not required to obtain the proper point-spread function, as it is in 2-D CT. Figure 2 illustrates the reconstruction obtained using nearest-neighbor interpolation for three different positions of the point object with respect to the reconstruction grid.

In the reconstruction process, it is assumed that the object remains stationary with respect to the reconstruction grid but that numerous projections are taken with various grid offsets y_0 . It can be shown that the resulting reconstruction $r^D(x)$ sampled at a spacing b has the Fourier transform

$$R^D(f) = A_{f_b} \{ H(f) G(f) P(f) e^{i2\pi\Delta f} \}, \quad |f| \leq f_b \quad (13)$$

where the Nyquist frequency for the reconstruction is $f_b = (2b)^{-1}$. It is interesting to note that the aliasing effects with respect to the projection Nyquist frequency have been removed by the averaging over all y_0 . However, since the reconstruction is itself

discretely sampled, the result is aliased with respect to the reconstruction Nyquist frequency. Similarly, the noise power spectrum of the reconstruction is

$$S_r^D(f) = (\text{NEQ})^{-1} A_b \{|H(f)|^2\} \quad (14)$$

Reconstruction SNR

The power SNR for the reconstruction is

$$\text{PSNR}_r^D(f) = \frac{|R^D(f)|^2}{S_r^D(f)} = \text{NEQ} \frac{|A_{f_b} \{ \text{HGP } e^{i2\pi\Delta f} \}|^2}{A_{f_b} \{|H|^2\}}, |f| \leq f_b \quad (15)$$

This equation is similar to that obtained for the projections, Eq. 10, but there are subtle differences. One of the most important features of Eq. 15 is that in the numerator it is the amplitudes which are aliased, not the power. Thus, the exponential phase factor for the position of the object Δ has a powerful effect upon the aliased result. Figure 3 shows the PSNR of the nearest-neighbor reconstructions given in Fig. 2. For $\Delta = 0$, the phase factor plays no role and the aliased contributions add constructively. The result is a flat PSNR indicative of the δ -function reconstruction. However, for $\Delta = 0.5$, the phase factor leads to destructive interference between the aliased contributions. Thus, the phase factor is crucial in accounting for the dependence of the reconstruction upon the object position.

Equation 15 is also different from Eq. 10 in that the interpolation transform $H(f)$ appears. However, if $H(f)$ were zero above f_b (band-limited), then the aliasing has no effect. The resulting PSNR would be the same as Eq. 10 except that it would not be aliased with respect to f_b . Thus, the net SNR (Eq. 3) would be the same, i.e., there would be no loss in SNR in the reconstruction process. One way to achieve this result is to use a very small sample spacing b for the reconstruction to make f_b large enough that $H(f)$ is arbitrarily small above f_b . Of course, this brute force method may not always be economically feasible, for example, in 2-D CT where from 100 000 to 260 000 computer words are routinely used to represent the reconstructions.

DQE and MTF

The detective quantum efficiency¹² (DQE) relates the power SNR subsequent to some stage of signal processing $\text{PSNR}_{\text{OUT}}(f)$ to that preceding that stage $\text{PSNR}_{\text{IN}}(f)$:

$$\text{DQE}(f) = \frac{\text{PSNR}_{\text{OUT}}(f)}{\text{PSNR}_{\text{IN}}(f)} \quad (16)$$

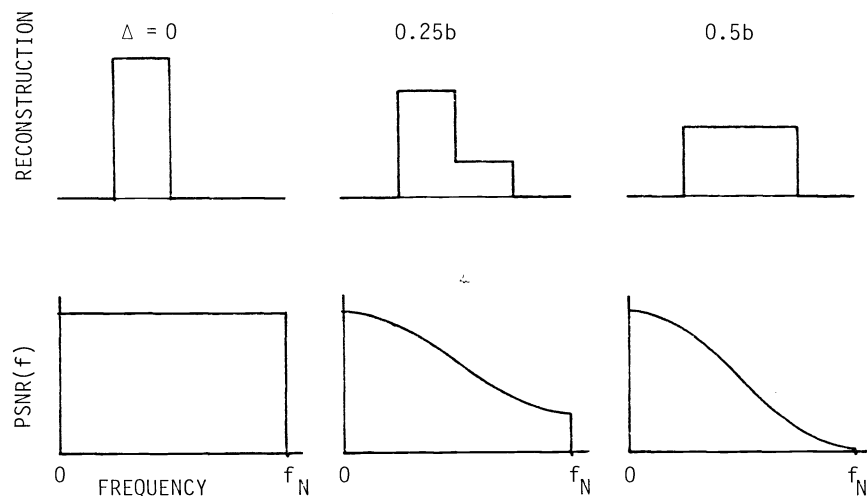


Fig. 3 The power signal-to-noise ratios (PSNR) corresponding to the reconstructions of Fig. 2 obtained with nearest-neighbor interpolation. The relative SNR's for the detection of the point object are 1, 0.79, and 0.71 for positions $\Delta/b = 0, 0.25,$ and 0.5 respectively.

Thus the optimum SNR for the detection of an object after processing is (Eq. 3)

$$\text{SNR}_{\text{OUT}}^2 = \int df \text{DQE}(f) \text{PSNR}_{\text{IN}}(f) \quad (17)$$

DQE is a convenient concept when applied to continuous coordinates since each stage of processing contributes multiplicatively to the net result. However, we see that the aliasing which occurs for discretely sampled signals renders the DQE concept unusable since the contributions at individual frequencies are no longer preserved. Further, as in Eq. 15, the aliasing can have different effects on the numerator and denominator of the PSNR and the effects in the numerator depend upon the Fourier transform of the signal, $P(f)$. Thus, it is impossible to separate PSNR_r into two factors as dictated by Eq. 17.

In the situation considered above in which $H(f)$ is assumed to be band-limited to f_b , we observed that the aliasing effects no longer exist and that the total SNR for the reconstruction is the same as for the projections. Thus, in some sense, the $\text{DQE}(f)$ for this case is 100%. It has already been shown² for reconstruction in continuous coordinates (which is an equivalent situation) that $\text{DQE}(f) = 100\%$. The import of this result is that an object may be detected in a band-limited reconstruction equally well as in the projection data themselves.

The modulation transfer function (MTF) or optical transfer function (OTF) concepts suffer the same deficiencies as DQE when applied to discretely sampled signals. While Eq. 13 gives the Fourier transform of the image, $P(f)$ cannot be separated from the expression as a multiplicative factor since the phase variation of $P(f)$ will affect the aliasing results. Another way of saying this is that the MTF of a system cannot be defined when the resulting image is not translation invariant. Of course, when the reconstruction becomes finely enough sampled that aliasing is eliminated, the reconstruction resolution may be legitimately characterized by the MTF.

Effective SNR

As noted above, the $\text{PSNR}(f)$ for the reconstruction may be a function of the position of the object relative to the reconstruction grid. It would be desirable to characterize the average effect of arbitrary or random positions of an object upon the detection capabilities inherent in the reconstruction. Let us consider as an example a situation in which a point object can only assume one of two positions, $\Delta = 0$ and $\Delta = 0.5b$. As shown in Fig. 3, the optimum SNR for the reconstructions will be either SNR_0 or 0.71SNR_0 , provided the observer is told the possible position of the object before making the decision. Suppose each of the two positions is equally probable. We would like to obtain the best possible ROC curve for this combined position case with an eye toward extension of the simple binary decision problem to the problem of the search¹³ where the position of the object is not known beforehand. Now, it is the probabilities for true positive and false positive responses which add linearly to obtain the combined ROC curve. The optimum ROC response which combines the best pairs of points from the ROC curves for the two possible object positions can be shown to belong to a different class than the individual ROC curves. That is, if the individual ROC curves characterize the performance obtained for additive, Gaussian noise, then the optimum combined ROC curve is not of the same form. In other words, the optimum decision function distribution will have non-Gaussian tails. Thus, the optimum combined response cannot be characterized by a single effective SNR.

While the foregoing considerations are true in general, the combined ROC curve can be approximately characterized by the average SNR:

$$\text{SNR}_{\text{eff}} = \sum_i P_i \text{SNR}_i \quad (18)$$

where P_i is probability that the object is in the i 'th position and SNR_i is the corresponding signal-to-noise ratio. This will be a good approximation when the individual SNR_i are not very different from one another or when the SNR_i are all small (≤ 1). When this is applied to the reconstruction method described in Fig. 2, the result of averaging over all possible object positions from $\Delta = 0$ to $\Delta = 0.5b$ is $\text{SNR}_{\text{eff}} = 0.81 \text{SNR}_0$ where SNR_0 is that for detection based on the projection data. It is seen that this reconstruction algorithm yields an average loss in SNR of 19%. Defining DQE as a summary measure (not a function of frequency any more):

$$\text{DQE} = \frac{\text{SNR}_{\text{eff}}^2}{\text{SNR}_{\text{in}}^2} \quad (19)$$

we find that the DQE of this reconstruction algorithm is 66%. This means that to achieve the same average detection capabilities for a point object in the reconstruction as in the projection data, the number of detected x rays must be increased by a factor of $(.66)^{-1} = 1.52!$

Let us consider an alternative reconstruction algorithm which uses linear interpolation in the backprojection process. As shown in Fig. 4, the result is to degrade the reconstruction for $\Delta = 0$. However, the SNR's for $\Delta = 0.25b$ and $0.5b$ are increased substantially. The effective SNR is found to be 0.87 SNR, and the corresponding DQE is 0.76. Note that although the reconstruction for $\Delta = 0.5b$ is the same as Fig. 3, the noise power spectrum is no longer constant (it is an aliased sinc⁴) leading to a higher PSNR.

From the above, we see that it is possible to alter the PSNR spectrum of the reconstructions by choosing various interpolation functions $h(x)$. If the principal application of the reconstruction is to facilitate the detection of point-like objects, then the interpolation function should be chosen to maximize the average detection sensitivity for a given amount of noise in the projections. It is well to point out that the choice of $h(x)$ may depend upon the aperture function $G(x)$. Thus, linear interpolation would appear to produce reconstructions superior to those produced by nearest-neighbor interpolation for the rectangular aperture assumed in Figs. 3 and 4. In practice, the choice of interpolation function should be tempered by practical considerations such as computation speed and appearance of the reconstruction (e.g., one might want to minimize ringing artifacts).

2-D Case

Backprojection

The filtered backprojection reconstruction algorithm¹⁴ used in two-dimensional CT can be seen to share many of the features of the one-dimensional model. In 2-D the discretely sampled projections must also be interpolated in the backprojection process. Figure 5 shows a set of projections which might be obtained for a point object. Suppose that the object happened to fall on the center of a reconstruction pixel. Then the positions at which the values of the projections must be known to obtain the backprojected value of that pixel are the same as the trajectory of the object. Near 0° it is seen that these positions do not always coincide with the projection sampling points. Rather, these positions actually are evenly distributed relative to the projection sampling points, much in the same way as occurred in the 1-D case through the variation in y_0 . Therefore, we expect that in the direction of these projections the 2-D reconstruction will be subject to the same effects as were uncovered in the 1-D model.¹⁵ Near 90° , on the other hand, the pixel position occurs repeatedly at the same position in the projections. Then for some small range of angles ($\sim 15^\circ$ in this case), no smoothing over projection position occurs. This leads to a reconstruction in these directions which more closely resembles the projections themselves.

The foregoing considerations indicate that all of the effects discussed in the 1-D model will be present to some extent in 2-D reconstruction. An additional complication in 2-D filtered backprojection is the effect of the $|f|$ filter required to remove the r^{-1} point spread function of simple backprojection. This filter must have a rather violent influence upon the reconstruction in the region close to the object. We might anticipate that this filter could affect the detection of small objects in 2-D, for example, because of inexact cancellation in the realm of discrete reconstruction.

Conclusions

It has been shown for a 1-D model that reconstruction in discrete coordinates from discretely sampled projections can lead to a loss of sensitivity for the detection of small objects. A similar loss of detection sensitivity is likely to occur in discrete 2-D CT reconstruction.

References

1. Hanson, K. M., "Detectability in the Presence of Computed Tomographic Reconstruction Noise," Proc. SPIE, 127, 304-312 (1978).
2. Hanson, K. M., "Detectability in Computed Tomographic Images," submitted to Medical Physics.
3. Wagner, R. F., Brown, D. G. and Pastel, M. S., "The Application of Information Theory to the Assessment of Computed Tomography," submitted to Medical Physics.
4. Joseph, P. M., "Image Noise and Smoothing in Computed Tomography (CT) Scanners," Proc. SPIE, 127, 43-49 (1977).
5. Tanaka, E. and Iinuma, T. A., "Correction Functions for Optimizing the Reconstructed Image in Transverse Section Scan," Phys. Med. Biol., 20, 789-798 (1975).
6. Tanaka, E. and Iinuma, T. A., "Correction Functions and Statistical Noises in Transverse Section Picture Reconstruction," Comput. Biol. Med., 6, 295-306 (1976).

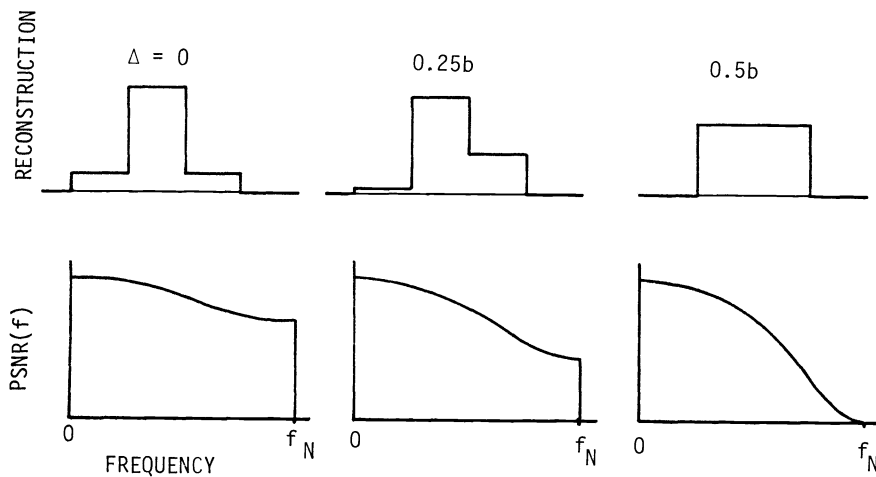


Fig. 4 Reconstructions obtained with the same projection data as Fig. 2 using linear interpolation and their corresponding PSNR's. The relative SNR's are 0.92, 0.87, and 0.80 for $\Delta/b = 0, 0.25$ and 0.5 respectively

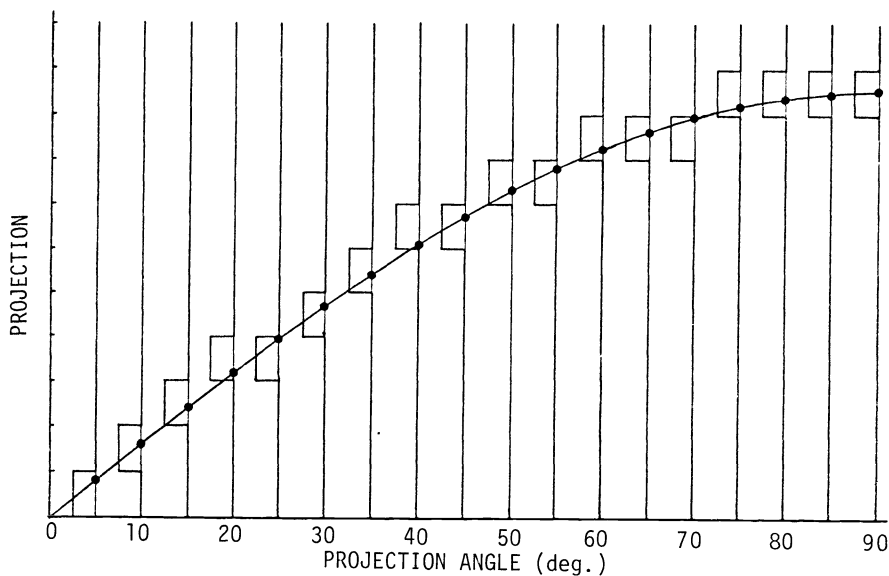


Fig. 5 Discrete projections of a point object for a rectangular aperture as a function of projection angle in 2-D.

References

7. Riederer, S. J., Pelc, N. J. and Chesler, D. A., "The Noise Power Spectrum in Computed X-Ray Tomography," *Phys. Med. Biol.*, 23, 446-454 (1978).
8. Davenport, W. B. and Root, W. L., *An Introduction to the Theory of Random Signals and Noise* (McGraw-Hill, NY 1958).
9. Whalen, A. D., *Detections of Signals in Noise* (Academic Press, NY 1971).
10. Brown, W. M., *Analysis of Linear Time-Invariant Systems* (McGraw-Hill, NY 1963).
11. Bracewell, R., *The Fourier Transform and Its Applications* (McGraw-Hill, NY 1965).
12. Dainty, J. C. and Shaw, R., *Image Science* (Academic Press, London, 1974).
13. Goodenough, D. J. and Metz, C. E., "Effect of Listening Interval on Auditory Detection Performance," *J. Acoust. Soc. Am.*, 55, 111-116 (1974).
14. Ramachandran, G. N. and Lakshminarayanan, A. V., "Three-Dimensional Reconstruction from Radiographs and Electron Micrographs: Application of Convolutions Instead of Fourier Transforms," *Proc. Natl. Acad. Sci. U. S.*, 68, 2236-2240 (1971).
15. Brooks, R. A., Glover, G. A., Talbert, A. J., Eisner, R. L., and DiBianca, F. A., "Aliasing - A Source of Streaks in CT Images," to be published in *J. Comp. Assist. Tomo.*